

Published in final edited form as:

*Analyst*. 2012 March 21; 137(6): 1402–1408. doi:10.1039/c2an16255e.

## Single molecule probes of membrane structure: Orientation of BODIPY probes in DPPC as a function of probe structure

Kevin P. Armendariz, Heath A. Huckabay, Philip W. Livanec<sup>†</sup>, and Robert C. Dunn  
Ralph N. Adams Institute for Bioanalytical Chemistry, University of Kansas, 2030 Becker Drive, Lawrence, KS, 66047

### Abstract

Single molecule fluorescence measurements have recently been used to probe the orientation of fluorescent lipid analogs doped into lipid films at trace levels. Using defocused polarized total internal reflection fluorescence microscopy (PTIRF-M), these studies have shown that fluorophore orientation responds to changes in membrane surface pressure and composition, providing a molecular level marker of membrane structure. Here we extend those studies by characterizing the single molecule orientations of six related BODIPY probes doped into monolayers of DPPC. Langmuir–Blodgett monolayers transferred at various surface pressures are used to compare the response from fluorescent lipid analogs in which the location of the BODIPY probe is varied along the length of the acyl chain. For each BODIPY probe location along the chain, comparisons are made between analogs containing phosphocholine and smaller fatty acid headgroups. Together these studies show a general propensity of the BODIPY analogs to insert into membranes with the BODIPY probe aligned along the acyl chains or looped back to interact with the headgroups. For all BODIPY probes studied, a bimodal orientation distribution is observed which is sensitive to surface pressure, with the population of BODIPY probes aligned along the acyl chains increasing with elevated surface pressure. Trends in the single molecule orientations for the six analogs reveal a configuration where optimal placement of the BODIPY probe within the acyl chain maximizes its sensitivity to the surrounding membrane structure. These results are discussed in terms of balancing the effects of headgroup association with acyl chain length in designing the optimal placement of the BODIPY probe.

### Introduction

The view of biological membranes and their functional role in cellular processes continues to evolve as new approaches are developed to probe these intricate structures. Biomembranes are composed of a complex mixture of lipids, proteins, sterols, and other species which combine to create highly heterogeneous and dynamic systems.<sup>1–5</sup> This often makes it difficult to directly link structural changes with membrane constituents, which has motivated the long historical development of model systems that mimic the natural cellular barrier. These simplified systems offer a high degree of control over important thermodynamic and compositional parameters. They have been essential in understanding natural membranes and developing and validating new tools for examining biological systems.

Fluorescence microscopy is one of the most widely used approaches for probing structural and dynamic attributes of both model and natural membranes. A wide variety of fluorescent

lipid analogs have been developed that readily insert into the macroscopic lipid assembly and often partition into particular domains, thus enabling heterogeneous structural features to be delineated. This approach has been used extensively to probe specific environments within lipid monolayers and bilayers, characterize phase structure, probe models of lipid rafts, and study the dynamics and fluidity of lipid membranes.<sup>6-9</sup> While fluorescence based analysis of membranes has been extensively developed and utilized, interpretation of the results and comparisons between studies is often complicated by the lack of detailed knowledge of probe/lipid interactions. For example, measured diffusion constants can vary by orders of magnitude, the assignment of dye partitioning within localized domains is often contradictory, and even the same fluorescent probe can alter its domain partitioning preference as a function of the lipid system composition.<sup>9-14</sup> This has renewed interest in understanding and controlling how probes insert into their target system.

There has been a considerable effort to design fluorescent probes capable of sensing the deep regions of membranes by positioning the fluorophore within the lipid acyl tails. For example, 1,6-diphenyl-1,3,5-hexatriene (DPH) has an elongated structure which is expected to insert along lipid acyl tails and has been widely used to probe order in the lipid tail region.<sup>15,16</sup> However, anisotropy measurements by Levine *et al.* have shown that DPH does not consistently insert as expected along lipid acyl tails but also inserts parallel to the membrane plane.<sup>17</sup>

Similar efforts have led to the development of lipid analogs incorporating the BODIPY fluorophore.<sup>18,19</sup> BODIPY probes are conceptually attractive for investigating the hydrophobic region of lipid membranes since they are less hydrophilic than other probes and have no net charge. BODIPY probes also exhibit excellent fluorescent properties with high extinction coefficients, near unity quantum yields, and favorable photo-stability properties.<sup>20,21</sup> In order to examine the incorporation of this fluorophore within the structure of lipid membranes, several studies have examined insertion properties of BODIPY lipid analogs located at incrementally longer regions of the acyl tail.<sup>22-25</sup>

Utilizing parallax analysis of fluorescence quenching, Kaiser and London have shown that while the average depth of the BODIPY fluorophore within the membrane is dependent on its position along the acyl tail, the BODIPY fluorophore also exhibits a broad distribution of locations within the membrane.<sup>24</sup> These results suggest that while the location of the BODIPY marker within the membrane generally tracks its location along the acyl chain of the probe, a significant population of fluorophores wrap back towards the headgroups and interact with the hydrophilic region of the membrane. Quenching studies in giant vesicles, moreover, found that essentially all of the BODIPY probes in the tailgroup looped back around to interact with the headgroups of the membrane, regardless of their location along the tailgroup.<sup>25</sup>

Clearly, the insertion geometry of BODIPY fluorescent membrane probes into lipid systems is complicated and requires further exploration using complementary techniques. Recently, we have shown that single molecule fluorescence measurements can characterize the orientation of individual fluorescent lipid probes doped into lipid membranes.<sup>26-30</sup> Using polarized total internal fluorescence microscopy (*P*-TIRFM), the three-dimensional orientation of fluorescent lipid analogs doped into films at trace levels can be characterized by emission pattern mapping. Using an acyl chain linked BODIPY-C<sub>4</sub>C<sub>9</sub>-PC probe, we have shown that these measurements are sensitive to membrane structure at the single molecule level. Variations in membrane structure induced by surface pressure changes, relative humidity, or additives such as cholesterol can all be tracked through changes in single molecule probe orientation. Moreover, these studies revealed a distinctive bimodal insertion geometry for the BODIPY-C<sub>4</sub>C<sub>9</sub>-PC probe, consistent with previous bulk studies of probe

orientations in membranes. These measurements, therefore, can compliment studies done on intact biological membranes and also provide molecular level details that help in their interpretation. For example, fluorescent lipid probes are often used for diffusion measurements in membranes which may be complicated by multiple insertion geometries.

Here we extend the previous studies to characterize the insertion geometry for a range of BODIPY lipid analogs in lipid films. In this study, the single molecule orientation distributions of six BODIPY fluorescent probes in DPPC Langmuir–Blodgett (LB) monolayers are examined. The BODIPY location in the acyl tail group is varied and analogs containing both phosphocholine (PC) and fatty acid (FA) headgroups are compared. These measurements are used to characterize how these probes insert and orient within DPPC monolayers and how their orientation changes with surface pressure. These studies reveal a general trend towards bimodal insertion geometries for BODIPY containing analogs. All six analogs reorient in response to changes in membrane surface pressure. The sensitivity to membrane surface pressure, however, is probe dependent and subject to the specific location of the BODIPY probe in the acyl tail and identity of the headgroup. These results, therefore, provide new insights into BODIPY containing probe insertion within membranes at the molecular level, which is important for interpreting results from bulk studies using these probes. The trends also provide guidance for the development of probes with increased sensitivity to changes in their surrounding lipid matrix. Together, these measurements illustrate the utility of single molecule fluorescence measurements for understanding the complicated and highly heterogeneous interactions that are indicative of membrane systems.

## Results and discussion

In previous studies, we have shown that defocused fluorescence imaging of individual BODIPY fluorescent lipid analogs doped into model membranes can elucidate structural changes in the lipid membrane at the molecular level.<sup>26–28</sup> These studies have been valuable for understanding how monolayer and bilayer systems may be influenced by factors such as surface pressure, humidity, and composition. To expand the capabilities of this approach and fully explore how probe orientations reflect membrane properties, here we analyze the single molecule orientations of a series of BODIPY-linked fluorescent lipid analogs doped into DPPC monolayers. The structures of DPPC and each of the fluorescent lipid analogs studied are displayed in Fig. 1. Each probe incorporates a BODIPY fluorescent marker within the acyl tail region of the lipid analog and is unique in terms of its fluorophore position along the acyl chain or headgroup type. These studies, therefore, will help establish the role of probe position and headgroup identity on insertion geometry in model membranes.

The emission dipole of the BODIPY marker lies approximately along the long axis of the fluorophore.<sup>20</sup> As shown previously, defocused P-TIRFM measurements enable characterization of the three-dimensional orientation of the emission dipoles from individual fluorescent lipid analogs doped into lipid membranes. These measurements, therefore, provide a direct visualization into the probe insertion geometry and can be used to track changes in the surrounding lipid matrix.

Each fluorescent marker was doped into DPPC monolayers at trace levels, compressed to the desired surface pressure on a Langmuir–Blodgett (LB) trough, and transferred to a glass coverslip for analysis. Deposition surface pressures ranged from 3 to 40 mN m<sup>-1</sup>; which span DPPC phase transitions from the predominantly liquid expanded (LE) phase, through the liquid expanded (LE)/liquid condensed (LC) coexistence region, to the predominantly liquid condensed (LC) phase. At low surface pressures, the DPPC monolayer is predominantly in the LE state which is characterized by a large area per lipid (>80 Å<sup>2</sup>/molecule at 20 °C), randomly oriented tailgroups, and reduced packing between the headgroups. As the

available area per molecule is reduced by compressing the membrane, the LC phase appears with tighter lipid packing ( $<60 \text{ \AA}^2/\text{molecule}$  at  $20 \text{ }^\circ\text{C}$ ), ordered acyl tails oriented away from the interface, and close packing of the lipid headgroups.

To demonstrate the utility of defocused fluorescence imaging for determining single molecule orientations, emission pattern mapping of the BODIPY fluorophore is illustrated in Fig. 2. The figure displays examples of experimentally measured emission patterns observed for a range of BODIPY orientations. Each example is compared with simulated emission patterns using previously describe approaches, where the only adjustable parameters are the polar ( $\phi$ ) and azimuthal ( $\theta$ ) angles of the BODIPY emission dipole and defocus distance.<sup>26</sup> The extracted emission dipole orientations are shown schematically in Fig. 2.

By comparing measured single molecule emission patterns with simulated results, orientation histograms are constructed to characterize the insertion geometry for each fluorescent marker shown in Fig. 1. In particular, the polar ( $\phi$ ) angle or tilt angle defines the extent of BODIPY tilt away from the surface normal and is used to describe the effective ordering of the BODIPY probe within the acyl tails of the DPPC monolayer as a function of surface pressure.

Fig. 3 shows representative defocused single molecule fluorescence images of BODIPY- $\text{C}_4\text{C}_9\text{-PC}$  doped at  $\sim 10^{-8}$  mol % into DPPC monolayers deposited at increasing surface pressures. Analysis of the single molecule emission patterns enables quantification of each individual orientation which is shown schematically in the center panels of Fig. 3. The polar ( $\phi$ ) or tilt angle of each emission feature is compiled to create tilt angle population histograms for each surface pressure as shown in the bottom panel of Fig. 3.

As previous single molecule studies have shown, molecular orientations of BODIPY- $\text{C}_4\text{C}_9\text{-PC}$  doped into DPPC films track changes in membrane ordering. Interestingly, consistent with the results shown in Fig. 3, these measurements reveal a bimodal distribution of orientations for BODIPY- $\text{C}_4\text{C}_9\text{-PC}$  doped into DPPC at all surface pressures studied. Significant populations of BODIPY- $\text{C}_4\text{C}_9\text{-PC}$  molecules were found to orient either normal ( $\phi = 10^\circ$ ) or parallel ( $\phi = 81^\circ$ ) to the membrane plane, with little population observed in the intermediate orientations. As shown in Fig. 3, as the surface pressure is increased, the population shifts towards the surface normal orientation with a concomitant decrease in the surface parallel orientation.

The bimodal distribution seen in Fig. 3 is consistent with a mechanism in which the lipid analog can insert into the DPPC membrane in an extended configuration with the BODIPY probe aligned along the lipid tails and a conformation in which the fluorophore wraps back to interact with the lipid headgroups. These configurations would lead to the normal oriented and parallel oriented populations, respectively. This is consistent with fluorescence quenching studies which found that the BODIPY probes tend to associate with the lipid headgroups even in condensed membranes.<sup>18,24</sup> While BODIPY is often described as a hydrophobic marker, distributed charge density within the ring system and charged resonance structures contribute to the observed hydrophilic nature of the BODIPY probe and its tendency to associate with membrane headgroups.

As shown in Fig. 3, the proportion of BODIPY- $\text{C}_4\text{C}_9\text{-PC}$  probes oriented normal to the membrane plane ( $\phi = 10^\circ$ ), which we term *ordered abundance*, increases with increasing surface pressure. The bimodal orientation distribution and trend towards increased ordered abundance at higher surface pressure is observed for all the BODIPY probes studied. Fig. 4 summarizes the single molecule orientation measurements for  $\text{C}_5\text{C}_9$ , and  $\text{C}_{12}$  BODIPY-PC and -FA probes in DPPC monolayers deposited at 3, 25, and  $40 \text{ mN m}^{-1}$ . The extracted ordered abundance-values for each of the probes are plotted as a function of surface pressure

in Fig. 4. Each point in Fig. 4 is extracted from single molecule population histograms such as that shown in Fig. 3, containing at least 450 molecules characterized from 3 different films. These plots clearly show that as the molecular area is reduced by compressing the monolayer to higher surface pressures, the ordered abundance for each probe studied increases linearly.

As shown in Fig. 4, the sensitivity with which each probe responds to increasing surface pressure, however, is dependent on head group type and BODIPY position along the acyl tail. Interestingly, the trends observed between BODIPY position and corresponding sensitivity to increasing surface pressure are not the same for PC and FA probes. The BODIPY-C<sub>4</sub>C<sub>9</sub>-PC probe exhibits the greatest sensitivity to changes in surface pressure compared to the other BODIPY-PC probes, while BODIPY-C<sub>12</sub>-FA shows the greatest sensitivity among the fatty acid probes examined. In addition, similar length PC and FA probes show statistically different sensitivities to surface pressure. The C<sub>5</sub> and C<sub>4</sub>C<sub>9</sub> FA analogs, for example, exhibit lower sensitivities to surface pressure compared with their PC counterparts, while only the C<sub>12</sub> FA analog exhibits higher sensitivity to surface pressure than its PC equivalent.

Several contributing factors may influence how the BODIPY probes insert into the membrane and thus influence their sensitivity to the changing lipid environment as the surface pressure is increased. The bimodal orientation distributions observed for all the BODIPY probes studied here is consistent with a general insertion model in which BODIPY probes aligned along the acyl chains lead to the normal oriented population ( $\varphi = 10^\circ$ ) while probes wrapped back towards the lipid headgroups give rise to the parallel oriented group ( $\varphi = 81^\circ$ ). In general, as surface pressure is increased and the area per lipid is reduced, the rise in normal oriented probes is consistent with an increasing population of BODIPY probes aligned along the acyl chains. Two primary factors, therefore, contribute to the probe insertion geometry; the order of the surrounding DPPC acyl tails and the probe proximity to the polar headgroups.

Before discussing the trends observed in Fig. 4, it is instructive to consider how the different headgroups affect the BODIPY location for similar length probes. Previous studies have shown that the position of fatty acid probes within membranes is strongly linked to pH.<sup>24,31</sup> Upon protonation and deprotonation, fatty acids can change depths within the membrane of up  $\sim 3$  Å. Given this, the fatty acid BODIPY analogs shown in Fig. 1 are expected to sit deeper within the DPPC headgroups than their PC counterparts, pulling the acyl attached BODIPY probe several angstroms closer to the surrounding lipid headgroups. As a first approximation, therefore, one would expect the relative probe depth of the BODIPY probes in the membrane to follow the general trend BODIPY-C<sub>5</sub>-FA < BODIPY-C<sub>5</sub>-PC < BODIPY-C<sub>4</sub>C<sub>9</sub>-FA < BODIPY-C<sub>4</sub>C<sub>9</sub>-PC < BODIPY-C<sub>12</sub>-FA < BODIPY-C<sub>12</sub>-PC.

Order within the surrounding DPPC acyl tails is necessary to induce order in the BODIPY probe and thus increase the abundance of  $\varphi = 10^\circ$  emission patterns. Evidence for this mechanism is provided by the trend that all PC and FA probes generally show an increase in ordered abundance with increasing surface pressure. NMR and molecular dynamics simulations show that the orientational freedom at each carbon along the acyl chain in a DPPC membrane is dependent on its distance from the headgroup.<sup>32,33</sup> These methods suggest that toward the end of the acyl tail (at approximately carbon 12 in DPPC) order begins to decrease rapidly with increasing distance from the headgroup, even at high surface pressures. Therefore, a lipid analog which places the fluorescent marker towards the end of the acyl tails in the monolayer will exhibit a decrease in ordered abundance compared to shorter probes due to a lack of rigidity from the surrounding acyl chains. In Fig. 4, for example, the BODIPY-C<sub>12</sub>-PC probe is much less sensitive to changes in membrane surface

pressure than the shorter BODIPY-C<sub>4</sub>C<sub>9</sub>-PC probe. For the FA probes, however, the trend is complicated. The trends in Fig. 4 reveal that the BODIPY-C<sub>12</sub>-FA probe is marginally more sensitive to surface pressure than the shorter BODIPY-C<sub>4</sub>C<sub>9</sub>-FA probe which is the reverse from that observed with the PC probes. However, because FA probes sit deeper in the headgroups and pull the BODIPY probes several Ångstroms closer to the headgroups, these probes in practice place the BODIPY group in ordered regions of the acyl tails as discussed.

The second factor considered to influence BODIPY insertion geometry is probe-headgroup electrostatic attraction given the charged resonance structures of the BODIPY probe. Probes located closer to the phosphocholine headgroups are more affected by this attraction and will have a greater resistance to orient along the acyl tails. Thus, probes linked with shorter acyl tails, such as the C<sub>5</sub> probes, are expected to exhibit lower sensitivity to acyl tail ordering with surface pressure since the BODIPY probe experiences stronger headgroup association. In Fig. 4, both the BODIPY-C<sub>5</sub>-PC and BODIPY-C<sub>5</sub>-FA probes exhibit the least sensitivity to changes in membrane surface pressure, consistent with this mechanism.

In general, the trends observed in Fig. 4 suggest that fluorescent lipid analogs with probes located closer to the headgroups exhibit progressively lower sensitivities due to increased electrostatic attraction to the headgroup region, while probes located near the terminal end of the acyl chains show reduced sensitivities due to the lack of acyl chain order in this region. Thus, these effects suggest that lipid analogs can be optimally tuned by judicious placement of the BODIPY probe along the acyl tail to maximize its orientation sensitivity to the surrounding membrane structure. Clearly, the data in Fig. 4 shows that the BODIPY-C<sub>4</sub>C<sub>9</sub>-PC probe experiences the greatest sensitivity to changes in the membrane surface pressure. This suggests that its BODIPY probe is positioned such that it minimizes the electrostatic interactions with the lipid headgroups while keeping it in the ordered region of the acyl tails. Because the FA probes sit deeper in the headgroups, the trends observed in Fig. 4 suggest that probe lengths between BODIPY-C<sub>4</sub>C<sub>9</sub>-FA and BODIPY-C<sub>12</sub>-FA would maximize their sensitivity to the surrounding lipid matrix. The slight difference in sensitivities observed for comparable PC and FA probes in Fig. 4 is consistent with trends expected given the different depths at which the headgroups reside in the membrane. This also indicates that the extra acyl chain of the PC probes has little effect on probe insertion or reorientation with surface pressure. The studies presented here, therefore, suggest that bimodal insertion geometries for BODIPY lipid analogs are a general feature of this probe and the BODIPY position can be tuned to maximize their sensitivity to the surrounding lipid matrix.

## Experimental

Dipalmitoylphosphatidylcholine (DPPC) (Avanti Polar Lipids, Alabaster, AL) was obtained at >99% purity and used without further purification. Fluorescent lipid analogs 2-(4,4-difluoro-5,7-dimethyl-4-bora-3a,4a-diaza-*s*-indacene-3-pentanoyl)-1-hexadecanoyl-*sn*-glycero-3-phosphocholine (BODIPY-C<sub>5</sub>-PC) (D-3803), 2-(5-butyl-4,4-difluoro-4-bora-3a,4a-diaza-*s*-indacene-3-nonanoyl)-1-hexadecanoyl-*sn*-glycero-3-phosphocholine (BODIPY-C<sub>4</sub>,C<sub>9</sub>-PC) (B-3794), 2-(4,4-difluoro-5,7-dimethyl-4-bora-3a,4a-diaza-*s*-indacene-3-dodecanoyl)-1-hexadecanoyl-*sn*-glycero-3-phosphocholine (BODIPY-C<sub>12</sub>-PC) (D-3792), 4,4-difluoro-5,7-dimethyl-4-bora-3a,4a-diaza-*s*-indacene-3-pentanoic acid (BODIPY-C<sub>5</sub>-FA) (D-3834), 5-butyl-4,4-difluoro-4-bora-3a,4a-diaza-*s*-indacene-3-nonanoic acid (BODIPY-C<sub>4</sub>, C<sub>9</sub>-FA) (B-3824), 4,4-difluoro-5,7-dimethyl-4-bora-3a,4a-diaza-*s*-indacene-3-dodecanoic acid (BODIPY-C<sub>12</sub>-FA) (D-3822) (Invitrogen Corporation, Carlsbad, CA) were used as received.

Lipid monolayers were prepared from 1 mg ml<sup>-1</sup> stock solutions of DPPC dissolved in chloroform and doped with ~10<sup>-8</sup> mol % of the appropriate reporter dye. The solutions were dispersed on a subphase of 18 MΩ water in a Langmuir–Blodgett trough (Type 611, Nima Technology, Coventry, England). The chloroform was allowed to evaporate for 15 min prior to beginning compression cycles. Each monolayer was subjected to two compression and expansion cycles up to a surface pressure of 40 mN m<sup>-1</sup>. Compression and expansion rates were 100 cm<sup>2</sup> min<sup>-1</sup> and 80 cm<sup>2</sup> min<sup>-1</sup>, respectively. Each monolayer was then compressed to a particular target pressure and held at that pressure for 10 min. The monolayer was then transferred to a Piranha-cleaned glass coverslip in a headgroup down geometry at a dipping speed of 5 mm min<sup>-1</sup>. All monolayers were transferred and studied at 22 °C.

Monolayer films were imaged using a total internal reflection fluorescence microscope (TIRF-M) (Olympus IX71, Center Valley, PA) equipped with a 100×, 1.45 NA objective (Achromat, Olympus). The 514 nm line from an argon ion laser (Coherent Innova 90, Santa Clara, CA) was directed through half-wave and quarter-wave plates (Newport, Irvine, CA) to select for p-polarized excitation before being coupled into the microscope. Excitation was directed through the objective with the optics defocused ~500 nm and fluorescence was collected, filtered, and imaged on a cooled CCD camera (Cascade 650, Roper Scientific, Tuscon, AZ). Image collection was controlled with Slidebook software (Version 4.2.0.3, Intelligent Imaging Innovations, Denver, CO) and analyzed with MATLAB (Natick, MA).

## Conclusions

Defocused polarized TIRF-M measurements were used to characterize the tilt angles of BODIPY containing fluorescent lipid analogs doped into DPPC monolayers. A total of six analogs are studied where the location of the BODIPY probe is varied along the acyl chain. Analogues with PC and FA head-groups are also compared with BODIPY probes located at comparable locations in the acyl tail. Each probe was doped into LB films of DPPC at ~10<sup>-8</sup> mol % and their single molecule orientations characterized over a range of surface pressures. For all probes studied, the single molecule tilt angle histograms reveal a predominately bimodal population distribution with probes oriented normal and parallel to the membrane plane. The bimodal tilt distribution is consistent with other studies that have shown BODIPY probes interact with both the acyl tails and lipid headgroups. The single molecule measurements reported here for a range of BODIPY probes suggest this is a general feature of membrane insertion for these lipid analogs. As the surface pressure of the film is increased, the population shifts from parallel to normal oriented probes for all the BODIPY analogs studied. The sensitivity to surface pressure, however, is shown to strongly depend on BODIPY location within the acyl tails and identity of the headgroup. The single molecule measurements suggest that analog structures which minimize BODIPY/lipid headgroup interactions while placing the BODIPY probe within structured regions of the acyl chains provides the optimal sensitivity to membrane surface pressure. Of the fluorescent lipid analogs studied here, the BODIPY-C<sub>4</sub>C<sub>9</sub>-PC probe demonstrated the highest sensitivity to membrane surface pressure changes. These results show that single molecule orientation measurements can help unravel the complicated interactions between fluorescent lipid probes and their surrounding membrane environments and provides a new tool for studying membrane structure and heterogeneity at the molecular level.

## Acknowledgments

K.P.A. gratefully acknowledges support from the NIH Dynamic Aspects of Chemical Biology Training Grant (T32 GM08545) and help from Esterenia Armanto. We thank Dr Jörg Enderlein for use of the MATLAB program used in the single molecule emission pattern modeling.

## References

1. Simons K, Ikonen E. *Nature*. 1997; 387:569–572. [PubMed: 9177342]
2. Brown DA, London E. *J. Membr. Biol.* 1998; 164:103–114. [PubMed: 9662555]
3. Shaw AS. *Nat. Immunol.* 2006; 7:1139–1142. [PubMed: 17053798]
4. Singer SJ, Nicolson GL. *Science*. 1972; 175:720–731. [PubMed: 4333397]
5. Silviu JR. *Biochim. Biophys. Acta, Biomembr.* 2003; 1610:174–183.
6. Burns AR, Frankel DJ, Buranda T. *Biophys. J.* 2005; 89:1081–1093. [PubMed: 15879469]
7. Frey SL, Chi EY, Arratia C, Majewski J, Kjaer K, Lee KYC. *Biophys. J.* 2008; 94:3047–3064. [PubMed: 18192361]
8. Dietrich C, Bagatolli LA, Volovyk ZN, Thompson NL, Levi M, Jacobson K, Gratton E. *Biophys. J.* 2001; 80:1417–1428. [PubMed: 11222302]
9. Gudmand M, Fidorra M, Bjørnholm T, Heimburg T. *Biophys. J.* 2009; 96:4598–4609. [PubMed: 19486682]
10. Schneider MB, Chan WK, Webb WW. *Biophys. J.* 1983; 43:157–165. [PubMed: 6616004]
11. Juhasz J, Davis JH, Sharom FJ. *Biochem. J.* 2010; 430:415–423. [PubMed: 20642452]
12. Baumgart T, Hunt G, Farkas ER, Webb WW, Feigenson GW. *Biochim. Biophys. Acta, Biomembr.* 2007; 1768:2182–2194.
13. Kahya N, Scherfeld D, Bacia K, Poolman B, Schwille P. *J. Biol. Chem.* 2003; 278:28109–28115. [PubMed: 12736276]
14. Kahya N, Scherfeld D, Schwille P. *Chem. Phys. Lipids.* 2005; 135:169–180. [PubMed: 15869751]
15. Parasassi T, Conti F, Glaser M, Gratton E. *J. Biol. Chem.* 1984; 259:14011–14017. [PubMed: 6548746]
16. Zannoni C, Arcioni A, Cavatorta P. *Chem. Phys. Lipids.* 1983; 32:179–250.
17. van der Heide UA, van Ginkel G, Levine YK. *Chem. Phys. Lett.* 1996; 253:118–122.
18. Boldyrev IA, Zhai X, Momsen MM, Brockman HL, Brown RE, Molotkovsky JG. *J. Lipid Res.* 2007; 48:1518–1532. [PubMed: 17416929]
19. Boldyrev IA, Molotkovsky IG. *Bioorg. Khim.* 2006; 32:87–92. [PubMed: 16523725]
20. Karolin J, Johansson LBA, Strandberg L, Ny T. *J. Am. Chem. Soc.* 1994; 116:7801–7806.
21. Johnson ID, Kang HC, Haugland RP. *Anal. Biochem.* 1991; 198:228–237. [PubMed: 1799206]
22. Omel'kov AV, Pavlova YB, Boldyrev IA, Molotkovsky JG. *Russ. J. Bioorg. Chem.* 2007; 33:505–510.
23. Sachl R, Boldyrev I, Johansson LBA. *Phys. Chem. Chem. Phys.* 2010; 12:6027–6034. [PubMed: 20390209]
24. Kaiser RD, London E. *Biochim. Biophys. Acta, Biomembr.* 1998; 1375:13–22.
25. Menger FM, Keiper JS, Caran KL. *J. Am. Chem. Soc.* 2002; 124:11842–11843. [PubMed: 12358515]
26. Livanec PW, Dunn RC. *Langmuir.* 2008; 24:14066–14073. [PubMed: 19053664]
27. Livanec PW, Huckabay HA, Dunn RC. *J. Phys. Chem. B.* 2009; 113:10240–10248. [PubMed: 19572622]
28. Huckabay HA, Dunn RC. *Langmuir.* 2011; 27:2658–2666.
29. Toprak E, Enderlein J, Syed S, McKinney SA, Petschek RG, Ha T, Goldman YE, Selvin PR. *Proc. Natl. Acad. Sci. U. S. A.* 2006; 103:6495–6499. [PubMed: 16614073]
30. Patra D, Gregor I, Enderlein J. *J. Phys. Chem. A.* 2004; 108:6836–6841.
31. Abrams FS, Chattopadhyay A, London E. *Biochemistry.* 1992; 31:5322–5327. [PubMed: 1606156]
32. Seelig A, Seelig J. *Biochemistry.* 1977; 16:45–50. [PubMed: 831777]
33. Song KC, Livanec PW, Klauda JB, Kuczera K, Dunn RC, Im W. *J. Phys. Chem. B.* 2011; 115:6157–6165. [PubMed: 21513278]



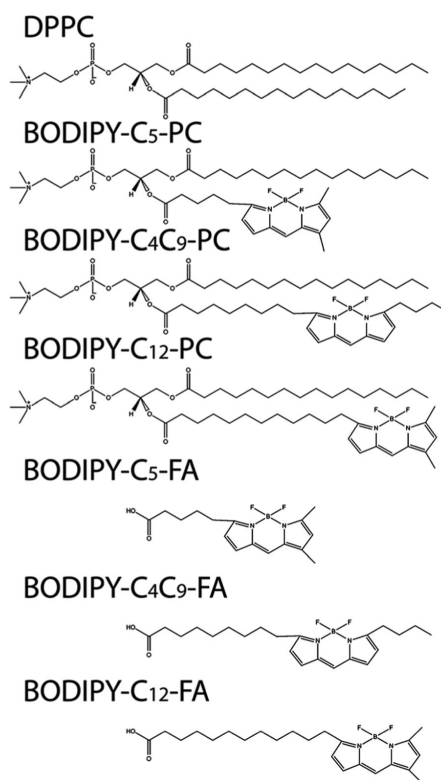


**Fig. 1.** Chemical structures for DPPC and the six BODIPY fluorescent lipid analogs studied. As shown by the structures, the BODIPY probe location in the acyl tail group is systematically varied and analogs containing both phosphocholine (PC) and fatty acid (FA) headgroups are compared in this study.

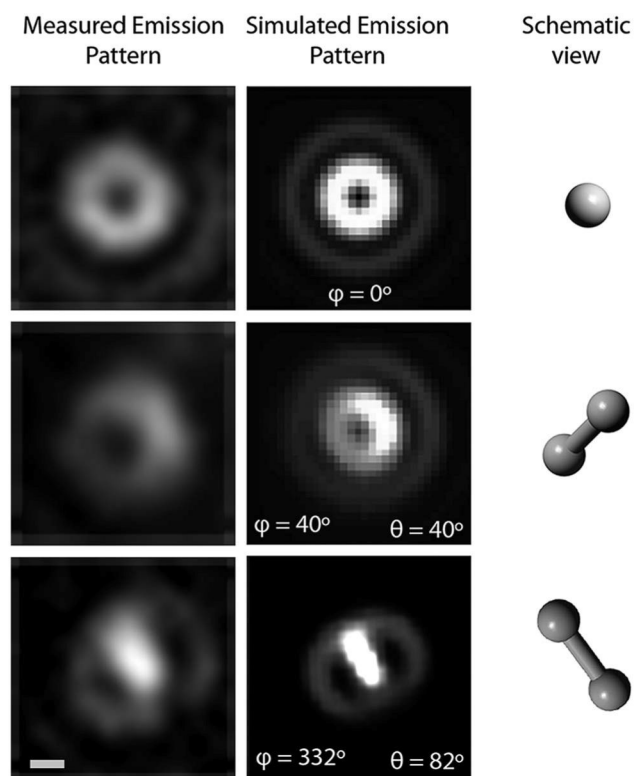


**Fig. 2.** **(Left)** Representative single molecule emission patterns measured using defocused polarized total internal fluorescence microscopy. **(Center)** Simulated emission patterns used to characterize the polar ( $\varphi$ ) and azimuthal ( $\theta$ ) angles of the BODIPY probe emission dipole. **(Right)** Schematic representations of the emission dipole orientations determined from the simulated emission patterns. The scale bar is 100nm.

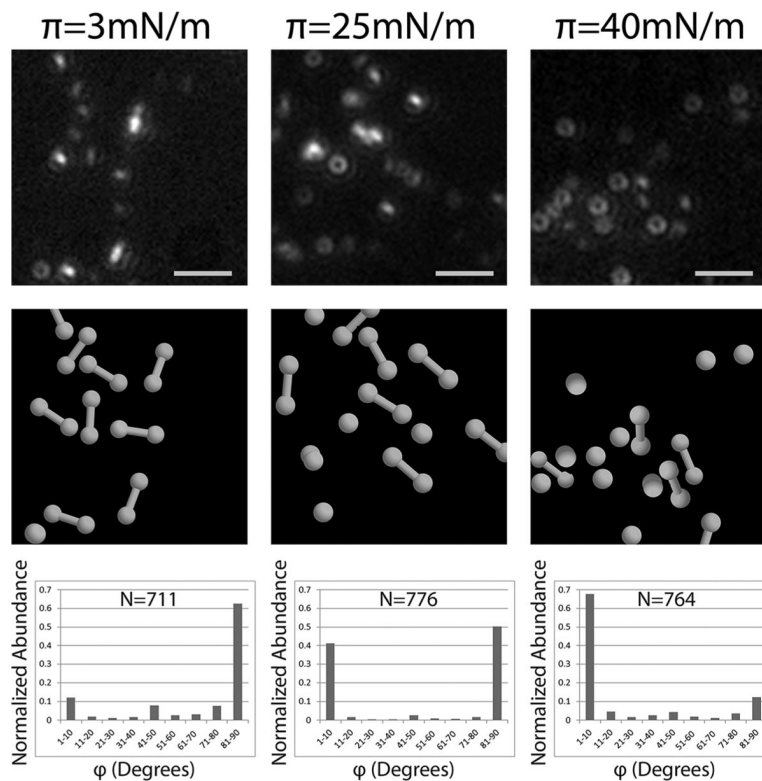


**Fig. 3.** (Top panels) Representative defocused single molecule fluorescence images of BODIPY- $\text{C}_4\text{C}_9\text{-PC}$  doped at  $\sim 10^{-8}$  mol % into DPPC monolayers deposited at 3, 25, and  $40\text{mN m}^{-1}$ . The scale bars are  $1\mu\text{m}$ . (Center panels) Schematics showing the single molecule orientations determined from simulating the single molecule fluorescence features measured in the top images. (Bottom panels) Polar ( $\phi$ ) or tilt angle histograms for BODIPY probes in DPPC monolayers transferred at the surface pressure indicated. Each histogram summarizes hundreds of individual tilt angles measured using the single molecule emission patterns collected at each film condition. The bimodal tilt distributions reveal large populations of BODIPY probes oriented normal ( $\phi = 10^\circ$ ) and parallel ( $\phi = 81^\circ$ ) to the membrane plane which shifts toward normal oriented probes as surface pressure increases.

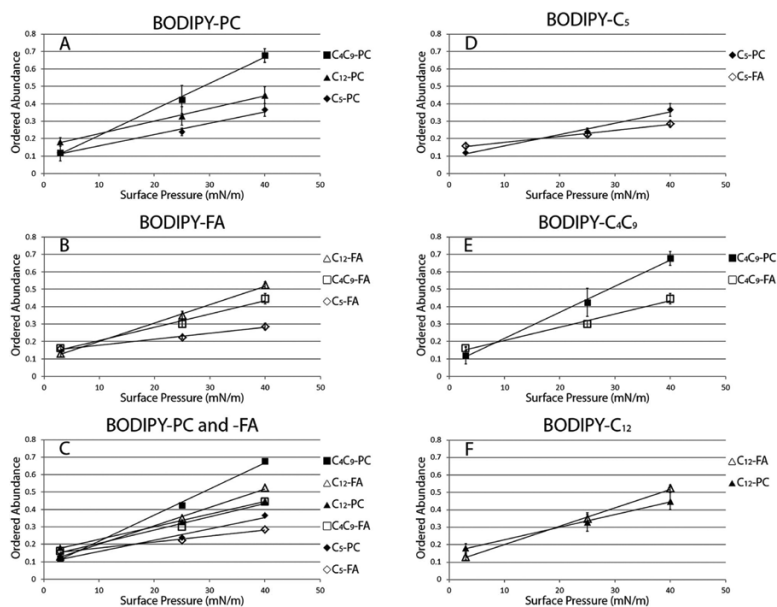


**Fig. 4.** Comparisons of the normalized population of normal oriented probes ( $\phi = 10^\circ$ ) as a function of DPPC surface pressure for the BODIPY probes shown in Fig. 1. Trends in the normal oriented BODIPY probes with (A) PC headgroups, (B) FA headgroups, and (C) all the probes studied are plotted as a function of surface pressure. (D–F) The populations of normal oriented probes *versus* surface pressure are plotted for lipid analogs that differ in headgroup but place the BODIPY probe in comparable positions along the acyl chain.